Applied Catalysis B: Environmental 162 (2015) 463–469

Contents lists available at ScienceDirect

Applied Catalysis B: Environmental

journal homepage: www.elsevier.com/locate/apcatb

Glucose–TiO_2 charge transfer complex-mediated photocatalysis under visible light

Gonu Kim[a], Sang-Hyup Lee[b,c], Wonyong Choi[a,*]

[a] School of Environmental Science and Engineering, Pohang University of Science and Technology (POSTECH), Pohang 790-784, South Korea
[b] Center for Water Resources Cycle Research, Korea Institute of Science and Technology (KIST), Seoul 136-791, South Korea
[c] Green School, Korea University, 145, Anam-ro, Seongbuk-gu 136-701, South Korea

ARTICLE INFO

Article history:
Received 29 May 2014
Received in revised form 8 July 2014
Accepted 13 July 2014
Available online 19 July 2014

Keywords:
Surface complex
Titanium dioxide
Ligand-to-metal charge transfer (LMCT)
Glucose
Visible light photocatalysis

ABSTRACT

Glucose adsorbed-TiO_2 nanoparticles show photoactivity under visible light ($\lambda > 420$ nm) through the ligand-to-metal charge transfer (LMCT) mechanism. Although glucose has been often utilized as a hole scavenger in TiO_2-based photocatalytic systems, the fact that TiO_2–glucose can form a LMCT complex that absorbs visible light has not been recognized. The TiO_2–glucose LMCT complex induced a marked red-shift in the absorption spectrum which extended to 600 nm, and the visible light absorption gradually decreased with decreasing the concentration of glucose. The TiO_2–glucose complex exhibited remarkable visible light activities for the reduction of Cr(VI) to Cr(III) and the reduction of O_2 to H_2O_2. The observed visible light activities were significantly inhibited when the TiO_2 surface was fluorinated, because the surface fluorides inhibited the formation of LMCT complex of glucose. The electrode coated with TiO_2–glucose complex generated a significant level of photocurrent under visible light. The ATR-FTIR spectra showed that glucose forms a surface complex on TiO_2 through the hydroxyl linkages. The evidences for the formation of the TiO_2–glucose complex and the experimental parameters affecting the visible light-induced activities are discussed in detail.

© 2014 Elsevier B.V. All rights reserved.

1. Introduction

Titania with a wide bandgap (3.0–3.2 eV) has been commonly used as a photocatalyst for environmental remediation and solar energy conversion [1]. Various methods are being investigated intensively to make TiO_2-based photocatalysts work under the visible light. One of the most popular approaches to overcome this problem is the dye sensitization [2]. In the dye sensitization, visible light is absorbed by the dye itself, and the photoexcited electron in the dye is transferred to conduction band (CB) of TiO_2. However, most of successful dye sensitizers are inorganic complexes of expensive/toxic metals such as ruthenium bipyridyl derivatives [3–5].

Another type of sensitization is the surface complexation of ligand-to-metal charge transfer (LMCT). In the LMCT sensitization, electron is photoexcited directly from the highest occupied molecular orbital (HOMO) level of the adsorbate to the TiO_2 CB [6]. Therefore, the light absorption mechanism for the LMCT sensitization is different from that of dye sensitization. LMCT allows visible light absorption even when the adsorbate itself does not absorb visible light at all. The LMCT complexation is an easy way to extend light respond of TiO_2 to the visible region and is versatile because numerous adsorbates are potential candidates for the LMCT sensitization. A variety of organic or inorganic compounds that can form LMCT complexes on TiO_2 has been recently reviewed [6]. The TiO_2–catechol complex, for example, exhibits new absorption band with a tail extending to around 600 nm [7]. A theoretical study revealed that the visible spectral band of TiO_2–catechol complex is resulted from the LMCT and not significantly involved the lowest unoccupied molecular orbital (LUMO) state of catechol [8]. Zhang et al. demonstrated that the use of phenolic resin instead of monomeric phenol for the LMCT complexation on TiO_2 can make a stable LMCT complex that works under visible light [9]. Lao et al. investigated the degradation of persistent organic contaminant, Linuron, in the TiO_2–H_2O_2 system under visible light [10]. Li et al. proved the generation of hydroxyl radical in the visible light-irradiated TiO_2–H_2O_2 system by EPR analysis [11]. Many other compounds that were reported to form the LMCT complexes on TiO_2 include 4-chlorophenol [12], toluene 2,5-diisocyanate (TDI) [13,14], benzylic alcohols [15], fullerol [16], calixarene [17], 8-hydroxyquinoline [18], ascorbic acid [19], dopamine [20], ethylenediaminetetraacetic

* Corresponding author. Tel.: +82 54 279 2283; fax: +82 54 279 8299.
E-mail address: wchoi@postech.edu (W. Choi).

http://dx.doi.org/10.1016/j.apcatb.2014.07.027
0926-3373/© 2014 Elsevier B.V. All rights reserved.

acid (EDTA) [21], aromatic hydrocarbons [22], and gallic acid [23]. All the above examples involve the formation of LMCT complexes on TiO_2 that are responsible for the observed visible light activity.

Glucose is a common bioresource and product of photosynthesis, which is renewable, non-toxic, inexpensive and carbon-neutral in its entire life cycle [24]. Since glucose can be employed as a "green" hole scavenger in photocatalysis, glucose and carbohydrate can be photocatalytically reformed to generate hydrogen over various modified TiO_2 under UV irradiation [25–29]. For instance, Fu et al. investigated the effects of experimental parameters on H_2 evolution in the noble metal-loaded TiO_2 system [26]. Bahruji et al. compared the photocatalytic reactivities of various alcohols on Pd/TiO_2 and showed that glucose has high reactivity in producing H_2 [27]. Xu et al. reported that the photocatalytic activity of H_2 production from biomass (including glucose) reforming can be enhanced by tuning the anatase–rutile phase structure of Pt/TiO_2 [28]. Here we report that the glucose can form a LMCT complex on TiO_2 surface which exhibits the visible light activity. The TiO_2–glucose LMCT complex absorbs visible light significantly and exhibits visible light activity for the photoconversion of Cr(VI) and the production of H_2O_2 via O_2 reduction. In this work, the photocatalytic reactions of TiO_2–glucose complex under visible light were systemically investigated with varying experimental parameters. Evidences for the formation of charge transfer complex are also presented and discussed.

2. Experimental

2.1. Chemicals and catalyst preparation

TiO_2 (P25) with an average surface area of 50± $m^2\,g^{-1}$ and primary particle size of 20–30 nm was used as a base photocatalyst material. Chemical substrates used in this study are as follows: D-(+)-glucose (Sigma-Aldrich), D-(+)-maltose monohydrate (Sigma-Aldrich), cellulose (Sigma-Aldrich), D-(+)-glucosamine hydrochloride (Sigma-Aldrich), 2-deoxy-D-glucose (Sigma-Aldrich), 2-azido-2-deoxy-D-glucose (Sigma-Aldrich), sodium fluoride (NaF, Sigma-Aldrich), chloroplatinic acid ($H_2PtCl_6{\cdot}H_2O$, Aldrich), sodium dichromate dihydrate (Aldrich) as Cr(VI) reagent, 1,5-diphenyl carbazide (DPC, Sigma-Aldrich), acetone (Samchun), barium sulfate (Acros), lithium perchlorate (Aldrich), sodium nitrate (Sigma-Aldrich), sodium phosphate monobasic (Sigma-Aldrich), sodium phosphate dibasic (Samchun), *N*,*N*-diethyl-1,4-phenylene-diamine sulfate (DPD, Aldrich), peroxidase (Aldrich, type VI-A from horseradish). All reagents were used as received. Surface fluorinated TiO_2 (F–TiO_2) was prepared by adding 10 mM NaF to an aqueous suspension of TiO_2. Surface platinized TiO_2 (Pt/TiO_2) with a typical Pt loading of 1 wt% was prepared by using a photodeposition method as described previously [30]. Ultrapure (18 MΩ cm) deionized water was used and prepared by a Barnstead purification system.

2.2. Characterizations

The UV–visible absorption spectra of bare TiO_2 and glucose-adsorbed TiO_2 powder were obtained by employing a UV–visible spectrophotometer equipped with a diffuse reflectance attachment (Shimadzu UV-2600). The glucose-adsorbed TiO_2 powder was also characterized by attenuated total reflection Fourier transform infrared spectroscopy (ATR-FTIR) measurement. For the ATR-FTIR measurement, the powder samples were simply placed onto the ZnSe crystal and the spectra were collected (referenced against air). The ATR-FTIR spectra were recorded using a Thermo iS50 FT-IR spectrometer (resolution of 4 cm^{-1}) and 100 interferograms were added for each measurement.

The glucose-adsorbed TiO_2 powder samples for the measurements were obtained as follows. A calculated amount of glucose was added to aqueous TiO_2 suspension and the pH was adjusted at pH 3.5. When F–TiO_2 was used to see the effect of surface fluorination, NaF (10 mM) was added to the TiO_2 suspension. The glucose-adsorbed TiO_2 suspension was filtered, and then the obtained powder was dried in a vacuum oven at room temperature for over 1 day. The prepared samples were used for the diffuse reflectance UV–visible spectra (DR-UVS), ATR-FTIR measurement, and for the analysis of high-resolution transmission electron microscopy (HR-TEM, JEOL JEM-2200 FS).

2.3. Photcatalytic activity test and analysis

The TiO_2 powder (1 g L^{-1}) was suspended in a given concentration of glucose solution by simultaneous sonication and shaking for 30 s in an ultrasonic cleaning bath. The pH of the suspension was adjusted with $HClO_4$ or NaOH standard solution. All photoreactions were done after 30 min of adsorption equilibrium. For the photocatalytic activity tests, a 300-W Xe arc lamp (Oriel) was employed as a light source. Light was filtered through a 10-cm IR water filter and a cutoff filter, and then focused onto a 30-mL Pyrex reactor with a quartz window. During the reaction, the reactor was stirred magnetically. Sample aliquots were withdrawn from the reactor intermittently and filtered through a 0.45-μm PTFE syringe filter (Millipore) for analysis.

Photoconversion of Cr(VI) to Cr(III) was analyzed using a colorimetric method that uses 1,5-diphenylcarbizide (DPC) reagent. The color change at 540 nm ($\varepsilon = 4 \times 10^4$ L mol^{-1} cm^{-1}) was monitored using a UV–visible spectrophotometer (Agilent, 8453). Wavelength-dependent photocatalytic activities were investigated with using a set of long-pass cutoff filters ($\lambda > 420$, 455, 495, and 550 nm). The photogeneration of H_2O_2 was carried out under the same condition as that for the Cr(VI) reduction experiments except for the absence of Cr(VI) species. The concentration of photogenerated H_2O_2 was determined by a colorimetric DPD method [31]. All experiments were carried out in duplicate or triplicate sets to confirm the reproducibility under the identical experimental condition.

To determine the apparent photonic efficiency (APE) for the glucose-sensitized reduction of Cr(VI) and production of H_2O_2, the photocatalysis experiments were also carried out under the light illumination (from the Xe-arc lamp) filtered through an Oriel monochromator (centered at $\lambda = 430 \pm 10$ nm). The incident photon flux was measured using a Power meter (Newport 1830-C) and then converted into an incident photon flux (I_{in}), which was estimated to be 1.3×10^{-5} Einstein h^{-1} assuming the monochromatic wavelength of 430 nm. APE was determined as: $APE_{(H_2O_2)}(\%) = (2P_{H_2O_2}/I_{in}) \times 100$ where $P_{H_2O_2}(mol\ h^{-1})$ = the rate of H_2O_2 production, $APE_{(Cr(VI))}(\%) = (3P_{Cr(VI)}/I_{in}) \times 100$ where $P_{Cr(VI)}(mol\,h^{-1})$ = the rate of Cr(VI) reduction.

Generation of photocurrent was measured with using a TiO_2/FTO electrode immersed in an aqueous solution of glucose. The TiO_2/FTO electrode was fabricated as described elsewhere [32]. The TiO_2/FTO electrode, a Pt wire, and a Ag/AgCl electrode were used as a working, a counter, and a reference electrode, respectively. The electrolyte used was 10 mM $LiClO_4$, and argon gas was continuously purged through the aqueous solution. The photocurrent was measured with the application of potential bias of 0.5 V (vs. Ag/AgCl) using a potentiostat (Gamry, Reference 600) connected to a computer.

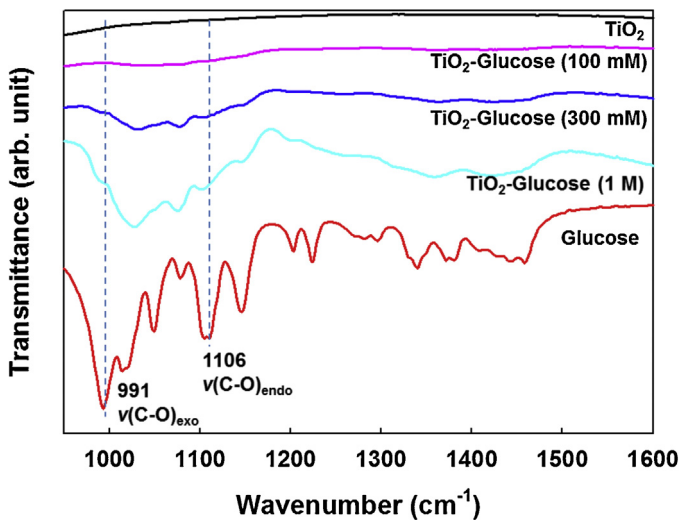

Fig. 1. ATR-FTIR spectra of bare TiO_2, pure glucose, and TiO_2–glucose powder samples.

3. Results and discussion

3.1. Formation of charge transfer complex and visible light absorption

Glucose has five hydroxyl groups that can bind to the TiO_2 surface. The complexation of glucose on the TiO_2 surface can occur through the condensation reaction between the hydroxyl group of glucose and the surface titanol group of TiO_2 (Eq. (1)). The formation of surface complex was investigated by ATR-FTIR spectroscopic measurements. For the purpose of comparison, the ATR-FTIR spectra of pure glucose and bare TiO_2 are shown in Fig. 1. Pure glucose has sharp characteristic bands at 991 cm^{-1} and 1106 cm^{-1}. The former one is ascribed to the stretching of exocyclic C—O group, while the latter one corresponds to the stretching of endocyclic C—O group [33]. With the TiO_2–glucose (1 M) sample, the band for the exocyclic C—O group was observed at 1027 cm^{-1}. Compared with pure glucose, the band position is shifted to a higher wavenumber, confirming the formation of surface complex through the hydroxyl group bound to the Ti center (Eq. (1)). The possible binding modes are illustrated in Scheme 1. When the concentration of glucose decreased from 1 M to 300 mM, the relative intensity for this $(C—O)_{exo}$ band is much more reduced than that of the $(C—O)_{endo}$ band which supports that the exo-band at 1027 cm^{-1} is attributed to the formation of TiO_2–glucose surface complex.

$$\equiv Ti(IV)—OH + HO—C_6H_7O(OH)_4 \rightarrow \equiv Ti(IV)—O—C_6H_7O(OH)_4 + H_2O \quad (1)$$

The TiO_2–glucose surface complex was directly observed with HR-TEM and electron energy loss spectroscopy (EELS) elemental mapping images. In Fig. 2, a thin carbon overlayer around the TiO_2 particle boundary was clearly observed in the EELS mapping images of the TiO_2–glucose (1 M) sample. The thickness of amorphous carbon overlayer on TiO_2 surface was about 1 nm (Fig. 2e), which roughly corresponds to the molecular size of glucose [34]. When compared to bare TiO_2 with some organic carbon impurities on its surface (Fig. 2f–h), the presence of carbon overlayer surrounding the TiO_2–glucose particles is outstanding.

The visible light absorption by the TiO_2–glucose surface complex was measured by DR-UVS. Fig. 3 shows the DR-UVS of pure glucose and TiO_2–glucose powders. Bare TiO_2 or pure glucose alone does not absorb visible light, but the TiO_2–glucose (1 M) powder absorbs significantly in the visible light region which extends up to around 600 nm. With decreasing the concentration of glucose, the visible light absorption gradually decreased, which supports the role of the TiO_2–glucose complex in the absorption of visible light. The color change was clearly observed upon adsorbing glucose on TiO_2 powder (see Fig. 3). When the surface of TiO_2 is fluorinated, the visible light absorption was markedly reduced because the presence of surface fluorides on TiO_2 inhibits the formation of charge transfer complex [35,36]. This reconfirms the formation of the glucose–TiO_2 charge transfer complex and its role in the visible light absorption.

3.2. Visible light activity of TiO_2–glucose charge transfer complex

The photoreduction of Cr(VI) to Cr(III) (Eq. (2)) and the production of H_2O_2 from O_2 reduction (Eq. (3)) under visible light was employed as probe reactions that investigated the electron transfer from the TiO_2–glucose complex (via TiO_2 CB) to electron acceptors (Cr(VI) or O_2) according to LMCT mechanism shown in Scheme 2.

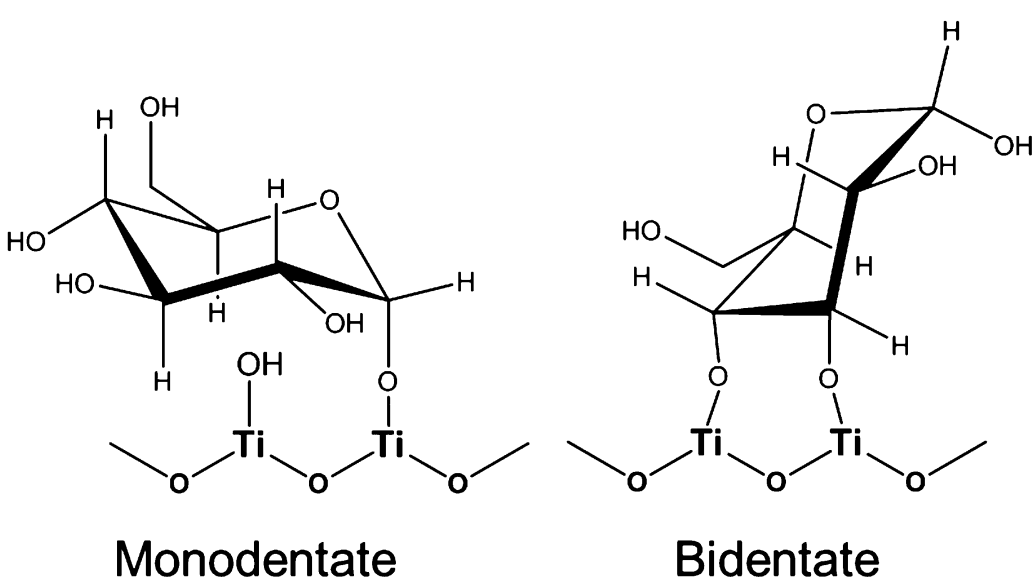

Scheme 1. Possible coordination structures of TiO_2–glucose complex.

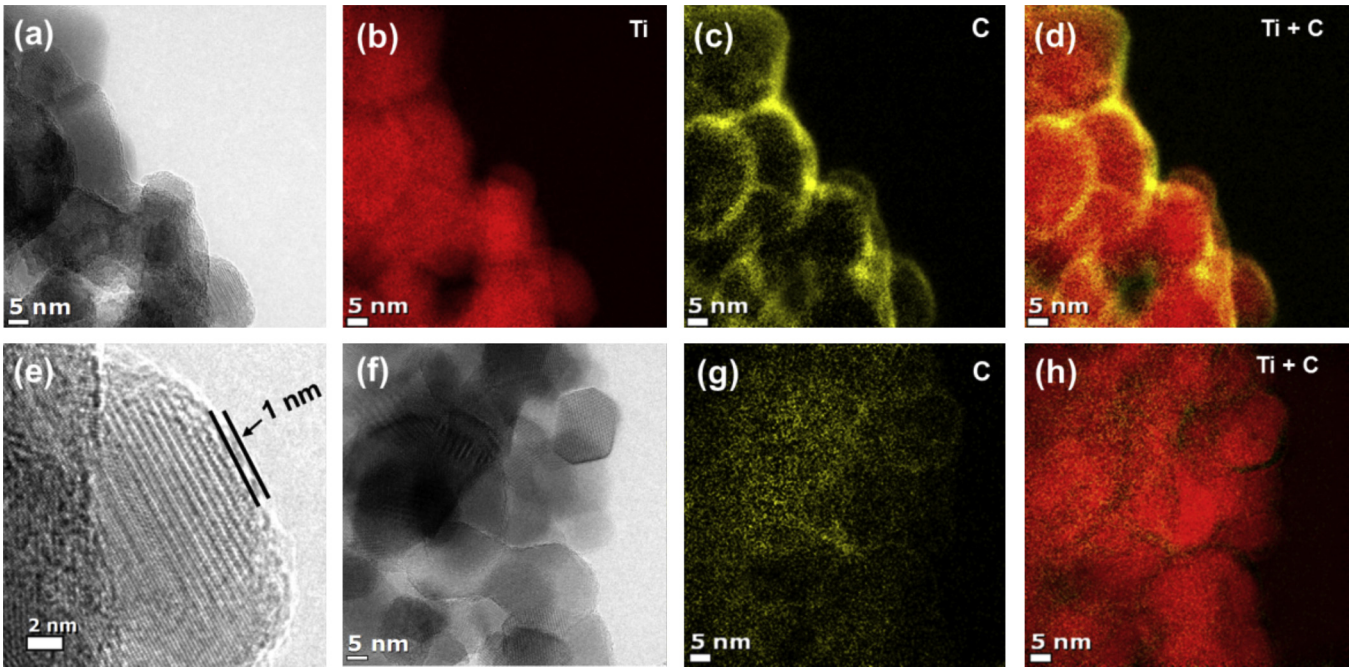

Fig. 2. (a) HR-TEM image of the TiO_2–glucose (1 M) sample. EELS elemental mapping of (b–d) Ti and C in TiO_2–glucose (corresponding to panel a). (e) HR-TEM image in a selected area in panel a. (f) HR-TEM image of the bare TiO_2. (g and h) EELS elemental mapping of Ti and C from impurity organics on bare TiO_2 (corresponding to panel f).

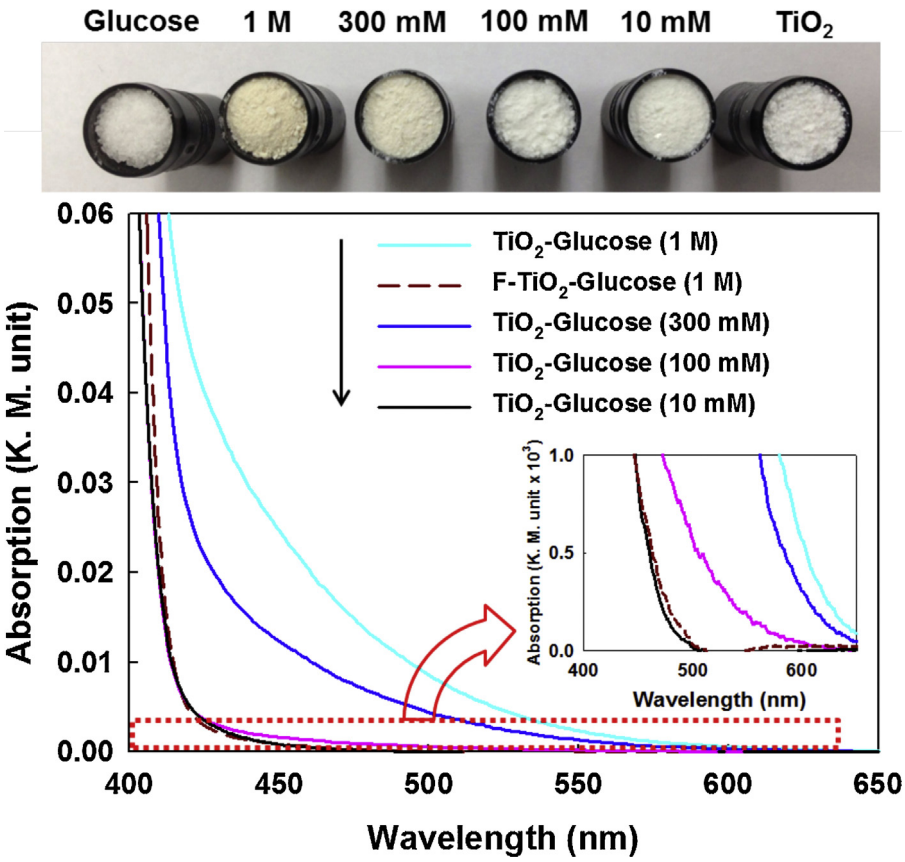

Fig. 3. Diffuse reflectance UV–visible spectra (DR-UVS) of the TiO_2–glucose powders with the reference taken as bare TiO_2 powder.

$$Cr_2O_7^{2-} + 14H^+ + 6e^- \rightarrow 2Cr^{3+} + 7H_2O(E^\circ = 1.36\,V_{NHE}) \quad (2)$$

$$O_2(g) + 2H^+ + 2e^- \rightarrow H_2O_2(E^\circ = 0.70\,V_{NHE}) \quad (3)$$

Fig. 4a shows that 100 μM of Cr(VI) can be completely removed within 40 min of visible light irradiation in the presence of TiO_2–glucose sample. Control experiments (without light, bare TiO_2, glucose alone) confirmed that the removal of Cr(VI) should not be ascribed to the dark complexation with glucose, the direct (photo)chemical reaction, nor the adsorption of Cr(VI) on TiO_2. With $[Glucose]_0 = 10$ mM, the apparent photonic efficiency (APE)

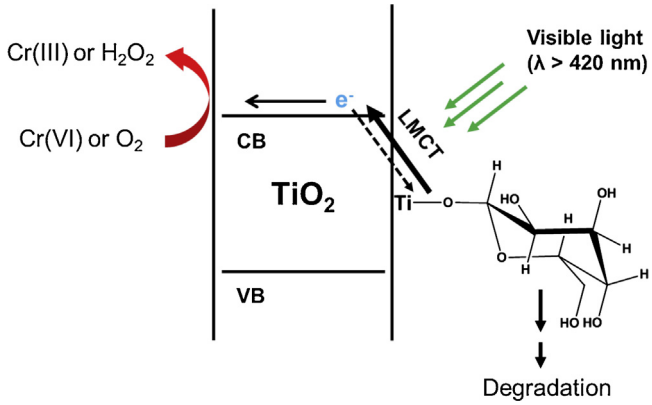

Scheme 2. Illustration of the visible light-induced photoreduction mechanism through the TiO_2–glucose LMCT complex.

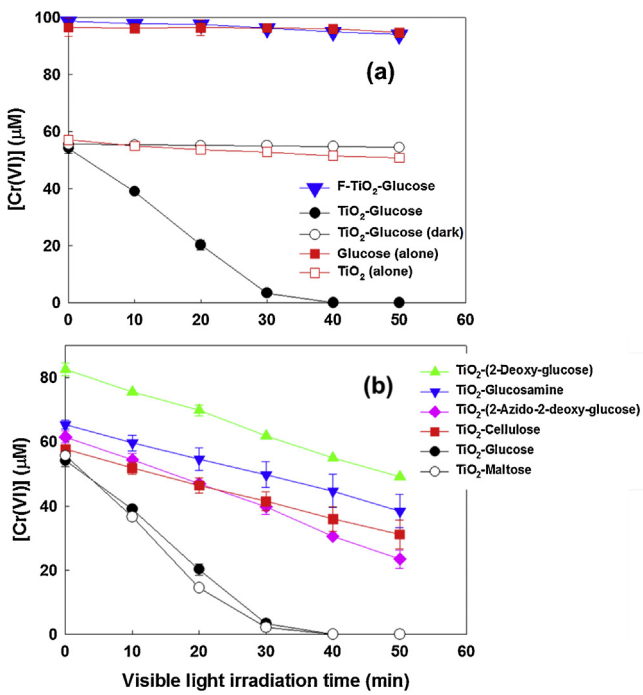

Fig. 4. Visible light-induced reduction of Cr(VI) on the glucose–complexed TiO_2. (a) the effect of surface modification of TiO_2 and (b) the effect of adsorbate (glucose derivatives) structure. The experimental conditions were $[TiO_2] = 1\,g\,L^{-1}$, pH 3.5, [Glucose or its derivatives] = 10 mM (in the case of cellulose, the same mass for 10 mM of glucose), $\lambda > 420$ nm, $[Cr(VI)]_0 = 100\,\mu M$, air-equilibrated.

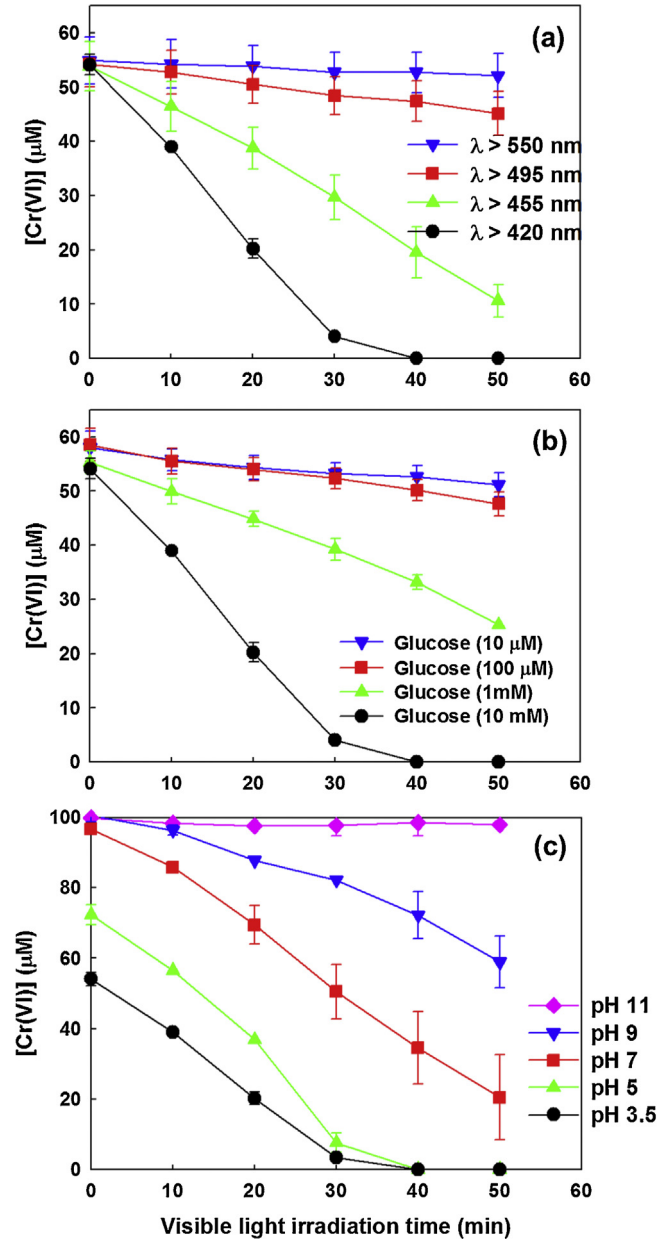

Fig. 5. (a) The irradiation wavelength-dependent and (b) glucose concentration-dependent and (c) pH-dependent photoreduction of Cr(VI) under visible light. The experimental conditions were $[TiO_2] = 1\,g\,L^{-1}$, [glucose] = 10 mM, $\lambda > 420$ nm, pH = 3.5, $[Cr(VI)]_0 = 100\,\mu M$, air-equilibrated.

at 430 nm for the Cr(VI) removal was estimated to be 4.5%. Since the glucose should serve as an electron donor for the reduction of Cr(VI), the glucose itself should be oxidized and degraded. However, we could not detect any sign of CO_2 generation nor the decrease of total organic carbon during the irradiation, which indicates that glucose was not mineralized but transformed into unidentified intermediates.

When the surface of TiO_2 was fluorinated, the complexation between glucose and the surface titanol group was hindered (as evidenced in Fig. 3), and as a result, the reduction of Cr(VI) was considerably inhibited. In Fig. 4b, the removal of Cr(VI) in TiO_2 suspension with other glucose derivatives was compared. When maltose, which is a disaccharide formed from two units of glucose, was used instead of glucose, Cr(VI) was also completely removed with 40 min of irradiation and the removal rate was almost similar to that of TiO_2–glucose complex. When cellulose, a polysaccharide consisting of a linear chain of glucose units, was tested for the Cr(VI) removal, about 30 μM of Cr(VI) was removed within 50 min of visible light irradiation. The Cr(VI) removal rate seems to be retarded with the TiO_2–cellulose complex probably because of the hindered LMCT complex formation (because of insolubility of cellulose in water) [37]. When 2-dexoy-D-gluose, glucosamine, and 2-azido-2-deoxy-glucose (which has the 2-hydroxyl groups replaced by hydrogen, amine group, and azido group, respectively) were examined, the substrate-adsorbed TiO_2 all exhibited significant visible light activity, but the reaction rates were lower than that of the TiO_2–glucose complex. The fact that the replacement of the hydroxyl group of glucose by other functional group reduced the visible light activity supports the critical role of the hydroxyl group in the formation of TiO_2–glucose LMCT complex.

The effects of wavelength of light, concentration of glucose, and pH on the photoreduction of Cr(VI) are shown in Fig. 5. The wavelength-dependent photoreduction of Cr(VI) was investigated

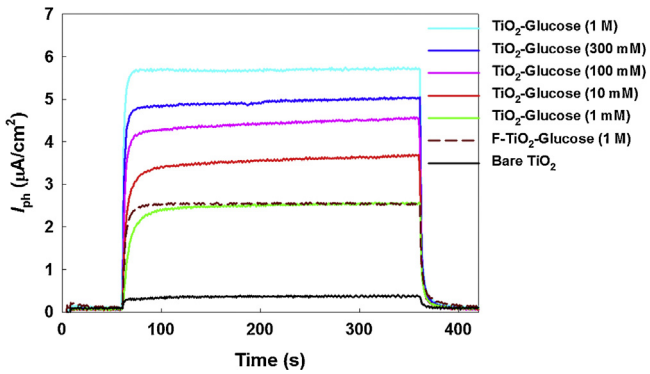

Fig. 6. (a) Time profiles of photocurrent generated with the TiO_2/FTO electrode in the visible light-irradiated aqueous solution of glucose. The experimental conditions were [$LiClO_4$] = 10 mM, pH = 3.5, λ > 420 nm, TiO_2/FTO electrode held at +0.5 $V_{Ag/AgCl}$, Pt wire counter electrode, continuously Ar-purged.

by using different long-pass cutoff filters to control the irradiation wavelengths (Fig. 5a). As the cutoff wavelength sequentially increased from 420 nm to 550 nm, the reduction rate of Cr(VI) rapidly decreased. This result is consistent with DR-UVS data in Fig. 3 which shows that the visible light absorption of TiO_2–glucose complex rapidly decreases with increasing the wavelength. When [Glucose] = 10 mM, the visible light absorption by the TiO_2–glucose complex vanishes at around 500 nm, and the reduction rate of Cr(VI) is almost negligible at λ > 550 nm. The agreement between the spectrum and photoactivity data indicates that the visible light activity of the TiO_2–glucose sample is clearly attributed to the LMCT excitation. A similar wavelength-dependent behavior for the photoreduction of Cr(VI) was also observed in the case of TiO_2–EDTA complex [21]. The concentration of glucose and pH also should affect the visible light activity of the TiO_2–glucose complex. As discussed in the previous section, the formation of the charge transfer complex and the corresponding visible light absorption should decrease as the concentration of glucose decreases. Therefore, the visible light activity of the TiO_2–glucose sample subsequently decreased as [Glucose] decreased from 10 mM to 10 μM (Fig. 5b). The effect of pH on the Cr(VI) reduction is shown in Fig. 5c. The initial reduction rate of Cr(VI) was not significantly influenced with increasing pH from 3.5 to 7.0, but gradually decreased above pH 7 and negligible at pH 11. The glucose complex formation should be hindered at high pH condition. In addition, the lower reduction rate of Cr(VI) at alkaline pH should be ascribed partly to the electrostatic repulsion between Cr(VI) anions and the TiO_2 surface. Since the surface charge of TiO_2 is mainly negative (pH_{zpc} ~6) at alkaline pH, the adsorption of Cr(VI) anions on the negatively-charged TiO_2 surface is inhibited [21,38]. The pH-dependent adsorption of Cr(VI) on TiO_2 is clearly seen when the concentration of Cr(VI) at time zero is compared in Fig. 5c: the equilibrated concentration of Cr(VI) prior to the light irradiation increased with raising pH from 3.5 to 11, which indicates that the Cr(VI) adsorbed on TiO_2 surface decreases with increasing pH. Consequently, the inhibited adsorption of Cr(VI) on TiO_2 at alkaline pH should retard the photoconversion of Cr(VI).

To elucidate the visible light-induced electron transfer from glucose to TiO_2 CB, the photocurrent generation was monitored with using TiO_2/FTO electrode immersed into the glucose-containing electrolyte solution. The generation of photocurrent in the presence of different $[Glucose]_0$ is compared in Fig. 6. The photocurrent results are consistent with DR-UVS and Cr(VI) photoconversion data. The TiO_2–glucose complexed electrode generated significant photocurrent under visible light, and the level of photocurrent decreased as $[Glucose]_0$ decreased. This photocurrent experiment provides a direct evidence for the electron transfer from the adsorbed glucose to TiO_2 CB under visible light.

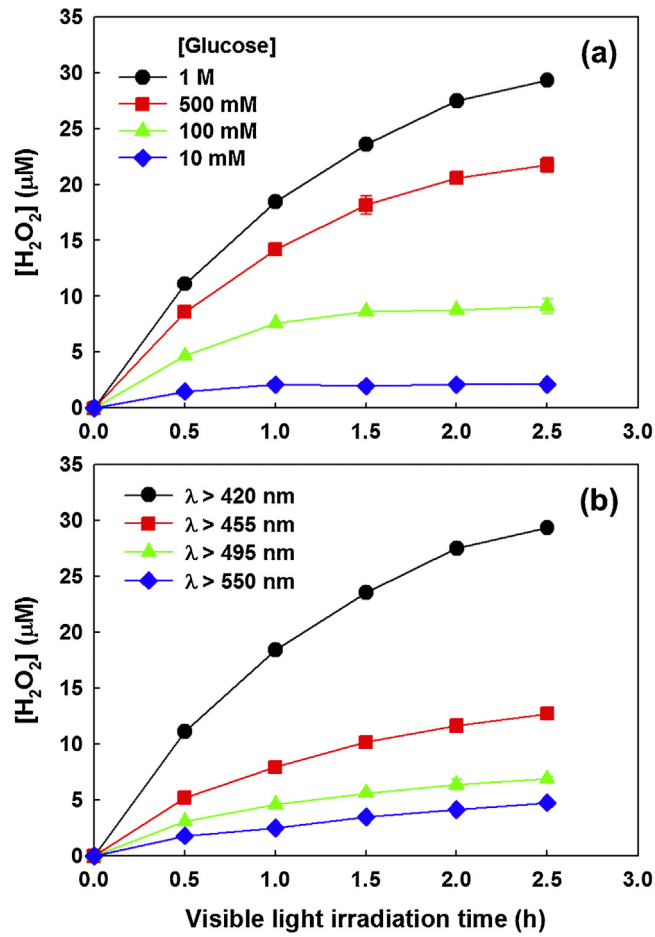

Fig. 7. (a) The glucose concentration-dependent and (c) irradiation wavelength-dependent production of H_2O_2 under visible light. The experimental conditions were [TiO_2] = 1 g/L, [Glucose] = 1 M, λ > 420 nm, pH = 3.5, air-equilibrated.

The visible light activity of the TiO_2–glucose complex was also examined for the generation of H_2O_2 through the photoreduction of O_2. Fig. 7a shows that the TiO_2–glucose (1 M) complex can produce a significant amount of H_2O_2 in an air-equilibrated suspension under visible light. The amount of H_2O_2 formed after 2.5 h of visible light irradiation was about 30 μM. As in the case of Cr(VI) removal experiment, the H_2O_2 production rate decreased with decreasing $[Glucose]_0$ (Fig. 7a), and decreased with increasing the cutoff wavelength (Fig. 7b). In control experiments in the absence of glucose or TiO_2, no H_2O_2 was generated, confirming that the phenomenon should be due to the formation of the LMCT complex. In the anoxic condition (Ar-purged suspension), no H_2O_2 was generated, which confirms that O_2 is apparently used as an electron acceptor for the reductive generation of H_2O_2. Compared with the Cr(VI) removal experiments, the H_2O_2 generation was achieved with much higher concentration of glucose. With $[Glucose]_0$ = 10 mM, the TiO_2–glucose complex removed 100 μM of Cr(VI) completely within 40 min of visible light irradiation (Fig. 4a), whereas it generated only about 2 μM of H_2O_2 from the reduction of ~250 μM of O_2 after 2.5 h of visible light irradiation (Fig. 7a) [39]. With $[Glucose]_0$ = 500 mM, the apparent photonic efficiency (APE) at 430 nm for the H_2O_2 production was estimated to be 0.61%, which is much lower than that for Cr(VI) removal (i.e., 4.5% with $[Glucose]_0$ = 10 mM). This is mainly ascribed to the fact that the reduction of Cr(VI) is thermodynamically more favored than that of O_2. (i.e., E_0 = 1.36 V_{NHE}, for Eq. 2 vs. E_0 = 0.70 V_{NHE} for Eq. (3)). Another reason for the low production efficiency of H_2O_2 might be the in-situ decomposition of H_2O_2 through a reductive pathway

($H_2O_2 + e^- \rightarrow HO\bullet + HO^-$) as soon as it is photogenerated on TiO_2 [40]. This indicates that the visible light activity of the TiO_2–glucose complex is significantly affected by the kind of electron acceptor, and the optimal reaction conditions for the LMCT sensitization should depend on the kind of photocatalytic reaction.

4. Conclusions

This study demonstrated that the glucose-adsorbed TiO_2 can form the charge transfer complex and exhibits visible light activity through the LMCT sensitization mechanism. Although glucose or TiO_2 alone cannot absorb the visible light, the TiO_2–glucose complex absorbs the visible light up to around 600 nm. The formation of TiO_2–glucose charge transfer complex was supported by ATR-FTIR spectra, EELS elemental mapping, and the photocurrent generation under visible light. The TiO_2–glucose complex apparently demonstrated the visible light activity for the photoconversion of Cr(VI) to Cr(III) and the production of H_2O_2 via O_2 reduction. The visible light-induced reaction was inhibited when the LMCT complex formation was hindered by surface fluorination. Beside glucose, glucose derivatives (2-dexoy-D-gluose, glucosamine, or 2-azido-2-deoxy-glucose) and other sugar alcohols (maltose, cellulose) also exhibited the visible light activities through the LMCT sensitization. Although the TiO_2–glucose complex cannot be used as a stable visible light sensitizer, because glucose should be degraded after the electron injection into TiO_2 CB, the visible light activity of TiO_2–glucose complex should be taken into account when glucose is present in TiO_2 photocatalytic systems (e.g., as a hole scavenger).

Acknowledgements

This work was supported by the Global Frontier R&D Program on Center for Multiscale Energy System (2011-0031571), KCAP (Sogang Univ.) (No. 2012M1A2A2671779) funded by the Korea government (MSIP) through NRF, and the Korea Ministry of Environment as “Converging Technology Project” funded by KIST (2011000600001).

References

[1] X. Chen, S.S. Mao, Chem. Rev. 107 (2007) 2891–2959.
[2] A. Hagfeldt, G. Boschloo, L. Sun, L. Kloo, H. Pettersson, Chem. Rev. 110 (2010) 6595–6663.
[3] Y. Cho, W. Choi, C.H. Lee, T. Hyeon, H.I. Lee, Environ. Sci. Technol. 35 (2001) 966–970.
[4] J. Park, J. Yi, T. Tachikawa, T. Majima, W. Choi, J. Phys. Chem. Lett. 1 (2010) 1351–1355.
[5] W. Kim, T. Tachikawa, T. Majima, W. Choi, J. Phys. Chem. C 113 (2009) 10603–10609.
[6] G. Zhang, G. Kim, W. Choi, Energy Environ. Sci. 7 (2014) 954–966.
[7] T. Lana-Villarreal, A. Rodes, J.M. Perez, R. Gomez, J. Am. Chem. Soc. 127 (2005) 12601–12611.
[8] P. Persson, R. Bergstrom, S. Lunell, J. Phys. Chem. B 104 (2000) 10348–10351.
[9] G. Zhang, W. Choi, Chem. Commun. 48 (2012) 10621–10623.
[10] Y.F. Rao, W. Chu, Environ. Sci. Technol. 43 (2009) 6183–6189.
[11] X. Li, C. Chen, J. Zhao, Langmuir 17 (2001) 4118–4122.
[12] S. Kim, W. Choi, J. Phys. Chem. B 109 (2005) 5143–5149.
[13] D. Jiang, Y. Xu, D. Wu, Y. Sun, Appl. Catal., B: Environ. 88 (2009) 165–172.
[14] F. Chen, W. Zou, W. Qu, J. Zhang, Catal. Commun. 10 (2009) 1510–1513.
[15] S. Higashimoto, N. Suetsugu, M. Azuma, H. Ohue, Y. Sakata, J. Catal. 274 (2010) 76–83.
[16] Y. Park, N.J. Singh, K.S. Kim, T. Tachikawa, T. Majima, W. Choi, Chem. Eur. J. 15 (2009) 10843–10850.
[17] J.M. Notestein, E. Iglesia, A. Katz, Chem. Mater. 19 (2007) 4998–5005.
[18] V.H. Houlding, M. Grätzel, J. Am. Chem. Soc. 105 (1983) 5695–5696.
[19] T. Rajh, J.M. Nedeljkovic, L.X. Chen, O. Poluektov, M.C. Thurnauer, J. Phys. Chem. B 103 (1999) 3515–3519.
[20] S. Varaganti, G. Ramakrishna, J. Phys. Chem. C 114 (2010) 13917–13925.
[21] G. Kim, W. Choi, Appl. Catal., B: Environ. 100 (2010) 77–83.
[22] Y.S. Seo, C. Lee, K.H. Lee, K.B. Yoon, Angew. Chem., Int. Ed. 44 (2005) 910–913.
[23] I.A. Jankovic, Z.V. Saponjic, E.S. Dzunuzovic, J.M. Nedeljkovic, Nanoscale Res. Lett. 5 (2010) 81–88.
[24] Y.-H.P. Zhang, Energy Environ. Sci. 2 (2009) 272–282.
[25] T. Kawai, T. Sakata, Nature 286 (1980) 474–476.
[26] X. Fu, J. Long, X. Wang, D.Y.C. Leung, Z. Ding, L. Wu, Z. Zhang, Z. Li, X. Fu, Int. J. Hydrogen Energy 33 (2008) 6484–6491.
[27] H. Bahruji, M. Bowker, P.R. Davies, L.S. Al-Mazroai, A. Dickinson, J. Greaves, D. James, L. Millard, F. Pedrono, J. Photochem. Photobiol., A: Chem. 216 (2010) 115–118.
[28] Q. Xu, Y. Ma, J. Zhang, X. Wang, Z. Feng, C. Li, J. Catal. 278 (2011) 329–335.
[29] N. Luoa, Z. Jiang, H. Shi, F. Cao, T. Xiao, P.P. Edwards, Int. J. Hydrogen Energy 34 (2009) 125–129.
[30] J. Lee, W. Choi, Environ. Sci. Technol. 38 (2004) 4026–4033.
[31] H. Bader, V. Sturzenegger, J. Hoigne, Water Res. 22 (1988) 1109–1115.
[32] H. Park, K.Y. Kim, W. Choi, J. Phys. Chem. B 106 (2002) 4775–4781.
[33] J.J. Max, C. Chapados, J. Phys. Chem. A 111 (2007) 2679–2689.
[34] S.J. Choi, B.G. Choi, S.M. Park, Anal. Chem. 74 (2002) 1998–2002.
[35] H. Park, W. Choi, J. Phys. Chem. B 108 (2004) 4086–4093.
[36] J. Kim, J. Lee, W. Choi, Chem. Commun. (2008) 756–758.
[37] R.P. Swatloski, S.K. Spear, J.D. Holbrey, R.D. Rogers, J. Am. Chem. Soc. 124 (2002) 4974–4975.
[38] Y. Ku, I.-L. Jung, Water Res. 35 (2001) 135–142.
[39] F.J. Millero, F. Huang, A.L. Laferier, Mar. Chem. 78 (2002) 217–230.
[40] I.K. Konstantinou, T.A. Albanis, Appl. Catal., B: Environ. 49 (2004) 1–14.